

Self-propelled chickpea harvester for small holding area

Mehdi Helali Soltan Ahmad*, Shamsollah Abdollahpour*, Hossein Navid

(Department of Biosystems, Faculty of Agriculture, University of Tabriz, Tabriz, 5166616474, Iran)

Abstract: Given the labor intensity of manual chickpea harvesting and the difficulty of using conventional cutterbar headers in rough and uneven fields, chickpea harvesting can turn into a costly and time-consuming process. For easier harvesting of chickpeas without these problems, the authors of this paper designed and fabricated a chickpea stripper header in accordance with the design principles of stripper headers and with attention to product characteristics and requirements. The components used in the design include a pneumatic collector and conveyer system, a pod accumulator, a cyclone separator, and a centrifugal fan. The mechanical power needed for rotating the header and the fan is taken from the engine of a BCS harvester, which is chosen because of its wide availability and practical features, in order to achieve good performance with reasonably low energy loss. After the design phase, the components were fabricated and assembled and the machine was subjected to preliminary assessments.

Keywords: chickpea, header, centrifugal fan, pod, stripper, conveyor

Citation: Soltan Ahmad, M. H., Sh. Abdollahpour, and H. Navid. 2023. Self-propelled chickpea harvester for small holding area. *Agricultural Engineering International: CIGR Journal*, 25(3): 95-108.

1 Introduction

Legumes can be harvested manually or by mechanized methods. The choice of harvesting method should be made with attention to the area under cultivation, field shape and slope, legume's type and cultivar, and planting method among other factors. Manual harvesting involves either cutting off pods with simple tools (e.g. a sickle, machete, or knife) or cutting the plant from its stem with bare hands (Arianpour, A., 2013).

Research conducted on the harvesting of chickpeas has shown that it is preferable not to remove the plant of this legume from the ground.

However, it is also practically impossible to harvest chickpeas from the stem by combine harvesters with common headers because some chickpea pods grow close to the ground and are therefore difficult to harvest without taking in gravel. Thus, stripper headers might be a better option for harvesting chickpeas. But common stripper headers also tend to be inefficient in harvesting chickpeas; an issue that can be attributed to the high spacing, low yield, and uneven growth and maturation of chickpea plants in the field. Hence, there is a need for a stripping mechanism more fitting to the specifications of this plant. Obviously, any proposed mechanism should be tested in the field under realistic conditions to ensure an appropriate level of reliability (Tavakkoli et al., 2009b).

To design a harvesting mechanism, it is crucial to know the shearing and cutting properties of the plant. These properties are measured experimentally, though they can also be derived from each other using theoretical methods.

1.1 Stem shearing force measurement for legumes

Received date: 2022-09-04 Accepted date: 2023-01-05

*Corresponding author: Mehdi Helali Soltan Ahmad, Department of Biosystems, Faculty of Agriculture, University of Tabriz, Tabriz, Iran. Tel: +98-914-7870619. Email: mehdihelali99@gmail.com.

Shamsollah Abdollahpour, Department of Biosystems, Faculty of Agriculture, University of Tabriz, Tabriz, Iran. Tel: +98-914-3156625. Email: shams@tabrizu.ac.ir

Stem shearing force needs to be measured to determine the amount of force required for harvesting the plant. This measurement can be done using the static method or the dynamic method. The static method involves placing the plant between two blades as in the harvester, applying increasing pressure on the blades by pouring water in an attached tank with an adjustable regulator until the stem is cut, and then measuring the weight of the water inside the tank (Abdollahpour et al., 2017). In the dynamic method, an electric motor is used to apply pressure as in the previous system, but the force is measured by a load cell with a strain gauge placed between the motor and the point of force application (Tavakkoli et al., 2009a).

1.2 Stripper headers

Research conducted in the United State and Italy has shown that using stripper headers instead of conventional headers can improve the harvest output by 50%-100% without increasing crop loss (West and Lundahl, 1986).

The first commercial stripper header was designed and manufactured in 1984 by the British company Shelbourne Reynolds Engineering Ltd. as an alternative to conventional headers attached in front of combine harvesters for better harvesting of various grains including wheat, barley, and rice. This header managed to improve the energy efficiency and field capacity of combine harvesters by 1.5 to 2 times (Metianu et al., 1991; Tado, 1992).

Jiang et al. (2001) fabricated a prototype stripper header with the ability to cut and line rice and wheat stems at high and low speeds. The tests conducted on this prototype showed that the grain loss can be reduced by the use of a pneumatic transmission system.

In Iran, Behroozi-Lar and Huang (2002) designed and fabricated a stripper header for harvesting chickpeas, which consists of eight rows of fingers installed longitudinally on its drum. This header, which is installed on the back of the tractor, is recommended for rain-fed fields.

Han et al. (2010) fabricated a stripper header

equipped with an air suction system for harvesting wheat and rice and investigated the effect of the forward speed, the linear velocity of the rotor teeth (peripheral speed), hood-to-rotor clearance, and the airflow velocity on harvesting loss. This investigation showed that the harvesting loss is significantly influenced by the peripheral speed, the forward speed, and the airflow velocity.

Chico-Santamarta et al. (2013) for the purpose of investigating the effect of airflow velocity and rotor rotation speed on the grain loss and efficiency of a stripper header, they designed three stripper fingers. Their results showed an increase in the header's stripping and threshing efficiency with the increase in the rotation speed of the stripper drum. These researchers stated that the grain loss can be reduced to an acceptable level by adjusting the airflow at the inlet and outlet of the header.

Bhanage et al. (2017) fabricated a stripper header for harvesting rice and investigated the effect of using two levels of forward speed (1.65 and 2.25 km h⁻¹) and four levels of peripheral speed (16.95, 19.78, and 22.6 and 25.45 m s⁻¹) on the header's shattered and unstripped grain loss. The field tests of this study showed that the shattered grain loss can be decreased by reducing the peripheral speed and increasing the forward speed.

Khojamli (2016) investigated the shattered and total grain loss of a stripper header equipped with a thresher unit and the effect of a series of independent variables on the header's grain loss and MOG in the tank. In this study, the lowest grain losses in the laboratory and field tests were 3.42% and 3.08% respectively, which were both achieved at a forward speed of 6 km h⁻¹, a rotational speed of 800 rpm, and a drum center height of 80 cm.

According to Firozi (2018), the desirable features of stripper headers include applicability in small farms, lower cost (compared to conventional headers), compatibility with high forward speeds, low grain loss, easy repair and maintenance, and structural simplicity.

The product harvested by the stripper header must

be transported to other components for further processing or storage as is the case with most combines. This transport is typically done by a system of conveyors.

2 Materials and methods

A chickpea harvesting machine was designed as per engineering design principles and with attention to common specifications of agricultural lands in Iran and the purchasing power of Iranian farmers, through the process shown in Figure 1.

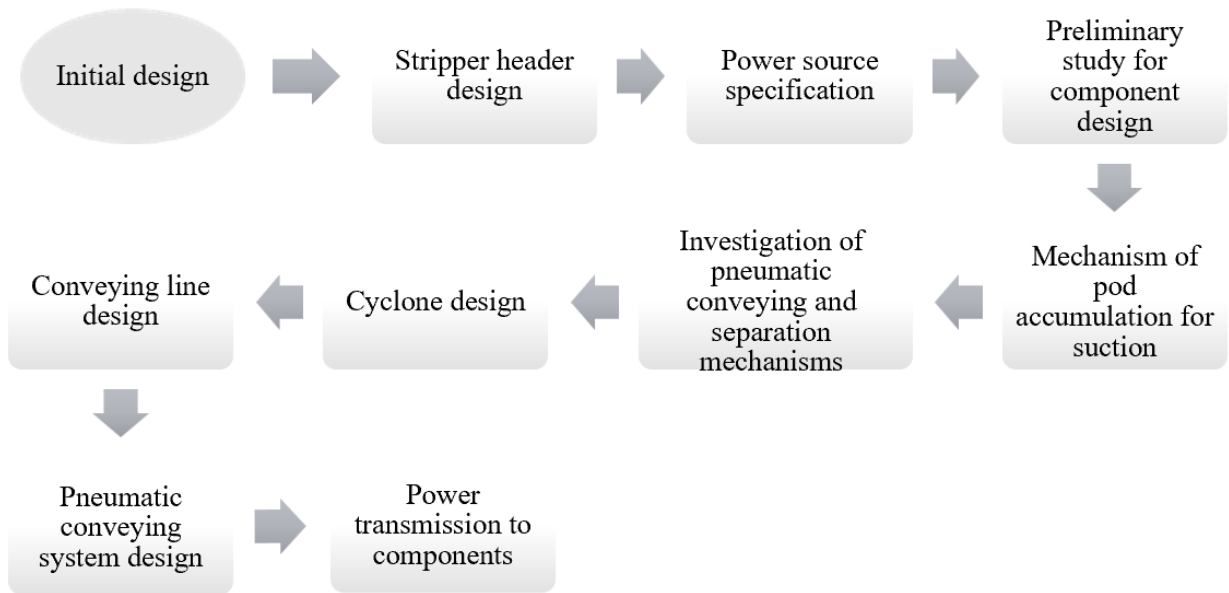


Figure 1 Block diagram of the research procedure

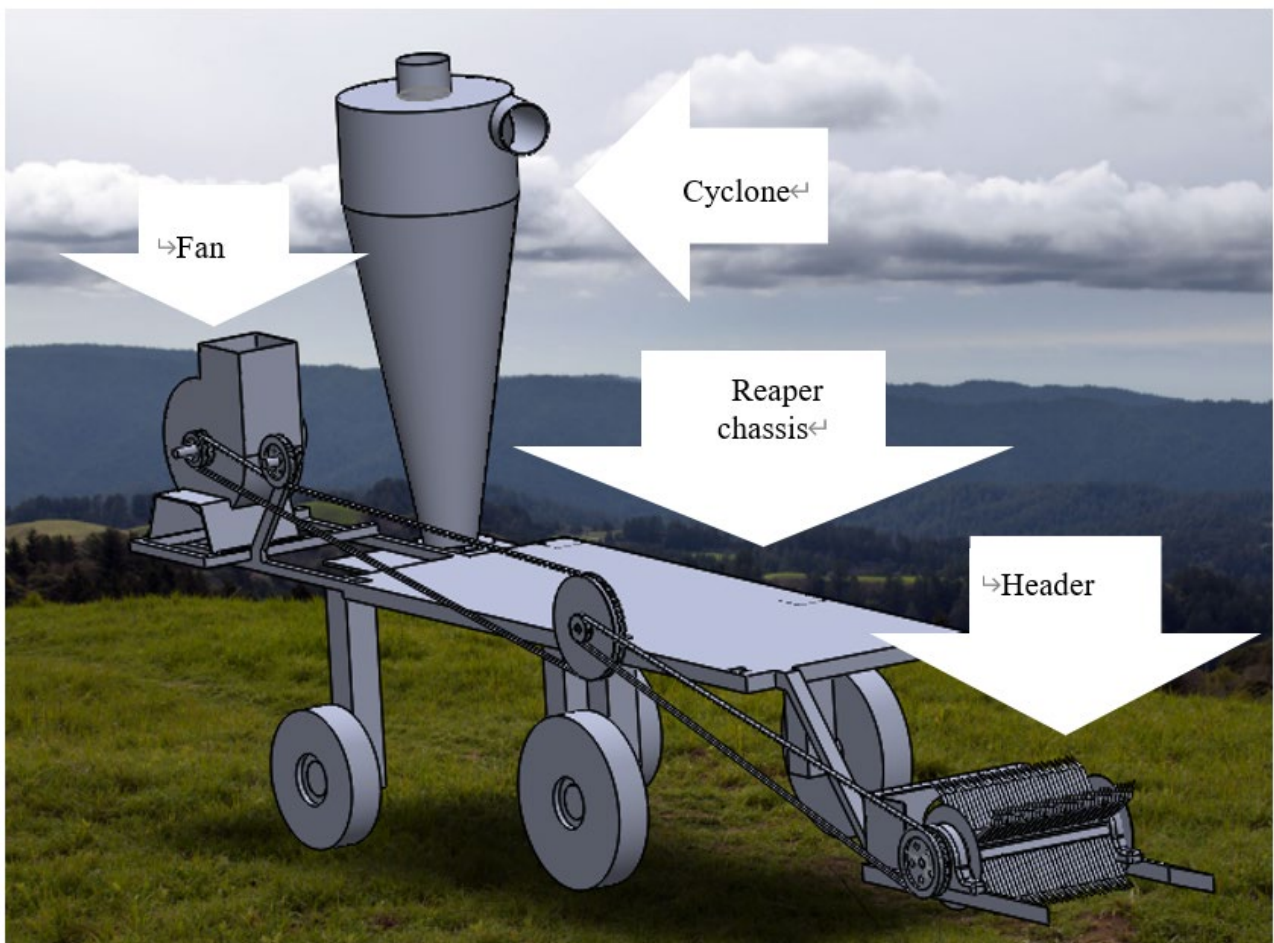


Figure 2 Schematic diagram of the machine and its components

2.1 Initial design

The model illustrated in Figure 2 was created in SOLIDWORKS based on the anticipated field requirements. A description of the component of this design and how they were chosen is provided in the following subsections.

2.2 Header

Considering the issues that make it difficult to harvest chickpeas with mechanized methods, including the short stature of the plant, potential unevenness of the field, and the dryness of the plant at the time of harvesting, the authors designed a new mechanism for harvesting chickpeas. Since it is practically impossible to harvest chickpeas with a

conventional cutter bar header, a stripper header was used in the machine.

Chickpea (Figure 3-A) is a small herbaceous, annual, long-day plant with hairy physic and a height of approximately 25-50 cm. Chickpea roots branch well into the soil to a depth of 1-2 m. A field where chickpeas are cultivated in regular rows (Figure 3-B). The plant's stem is straight, branching, cylindrical, and hairy. The leaves have a compound alternating structure about 5 cm length, consisting of 9-15 pairs of leaflets with a single leaflet at the end. The plant's fruit is a puffy and hairy pod containing 1-3 seeds. The 100-seed mass of chickpeas varies from 9 to 40 grams (Koochaki et al , 1986).



(A) Chickpea plant

(B) Chickpea land

Figure 3 Chickpea land and Chickpea Plant

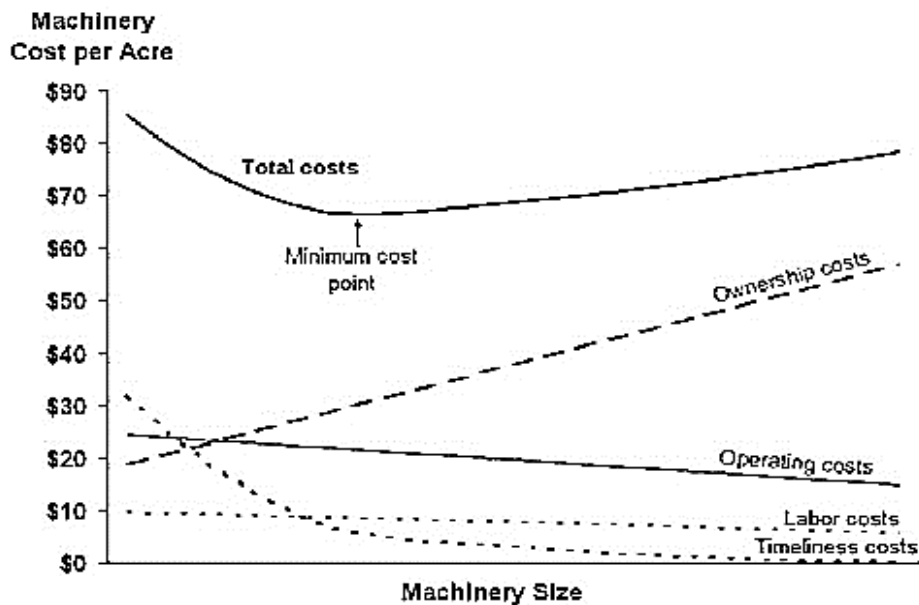


Figure 4 Machine size-related costs for a given farm

2.3 Power source

The choice of harvesting machine should be made with due attention to the field type and specifications.

For larger farms, it makes sense to use larger machines because although they are more expensive, they are also considerably faster and reduce the labor

cost by shortening the work duration. Otherwise, it is more economical to use small machines, unless the tardiness caused by slower harvesting would impose additional costs.

In addition to the aforementioned requirements, the power source must also be strong enough to power the machine components in preliminary assessments and offer good efficiency during work.

Therefore, as shown in Figure 4, the best machine size is the one that minimizes the sum of tardiness cost, machine cost, and labor cost (Behrouzilar, 2012).

BCS is a compact machine with a wide range of applications in farming including the harvest and sorting of wheat, barley, sesame, etc. The designed and fabricated header takes all of its required power from a BCS with a 12.5 HP engine, which meets the header's dimension and power requirements. This particular power source was chosen because of its low cost, wide availability in rural areas, and high

applicability and efficiency (especially the original brand).

2.4 Preliminary study for component design

To complete the design, a stripper head was designed and fabricated with the machine dimensions and components chosen based on design parameters (including geometric specifications, working conditions, and product properties). For the first time, a combination of a cyclone and a centrifugal fan with a dedicated mechanism was used to collect and accumulate the pods from the header for transport to a tank. The placement of the components for pod accumulation on the machine chassis, the dimensions and size of the cyclone and its placement in the machine, and the suction speed required for the centrifugal fan and its placement are discussed below.

Table 1 shows the physical properties and field conditions of chickpeas according to measurements.

Table 1 Properties of rain-fed chickpeas

Cultivar	Number of plants per unit area (m ²)	Number of pods per plant	Number of seeds per pod	Performance of rain-fed chickpeas	100-seed mass (g)	Plant height from the ground (cm)
Hashem		10.1	1.09	-	-	-
Grit	20	16.4	1.09	-	-	-
Karaj 31-60-12		12.8	1.09	-	-	-
Bionage						
Ilc482	33	10.22	1	799.72	28.11	-
Flip90-96						
Flip93-93						
ILC3279	-	8.91	-	520.6	29.2	23.8
Bahare	24	-	-	-	-	30-40

The working principle of the fabricated header is as follows: the rotating fingers at the front of the header comb the plant from the bottom, picking the pods as they carry the plant up, and then pour them into the accumulation component in the back as they go down. From there, the collected pods are sucked into the conveying system.

Considering the importance of the stripping area, field capacity, product inflow, and feed rate for each set of fingers, these parameters are discussed in more detail.

The stripping area is given by the following equation:

$$\text{Stripping Area (mm}^2\text{)} = \text{Header's working width (mm)} \times \text{Length of the finger touching the product (mm)} \quad (1)$$

Field capacity is the amount of work the machine accomplishes per hour. Thus:

$$F.C = \frac{V_s \times W_s \times \eta_f}{10} \quad (2)$$

where $F.C$ is the field capacity (ha h⁻¹) and V_s is the forward speed (km h⁻¹), W_s is the machine's working width (m), and η_f is the field efficiency.

$$n_c = N_{s.farm} \times v_m \times w_c \quad (3)$$

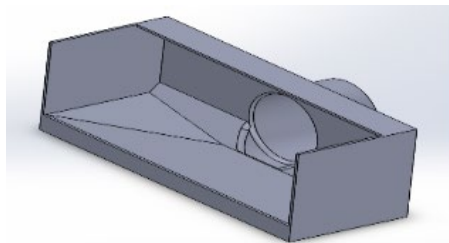
Where n_c is the number of stems taken in per

second, N_{s-farm} is the number of stems per unit area per second, v_m is the forward speed ($m\ s^{-1}$), and w_c is the width of the combine (m).

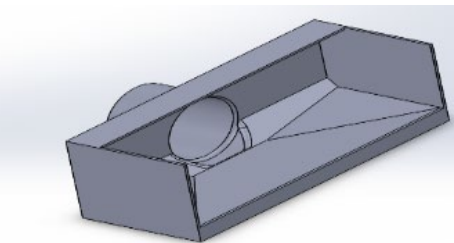
$$S_o = v_m t = v_m \frac{\theta}{\omega} = v_m \frac{2\pi}{\omega z} \quad (4)$$

Where S_o is the field capacity for a single row of teeth (m), z is the number of rows of teeth installed on the stripper drum (rotor), ω is the angular speed of the stripper drum ($rad\ s^{-1}$), t is the harvest duration of each row of teeth in one revolution of the stripper drum (s), and θ is the effective harvest angle of each row of teeth (rad).

2.5 Mechanism of pod accumulation and delivery



(A) Right perspective



(B) Left perspective

Figure 5 Schematic diagram of the accumulation component from the right and left perspectives

2.6 Pod transport (from stripper header to storage tank)

Agricultural products can be transported by a variety of methods, the choice of which depends on the nature, application, and phase of materials to be transported (fluid, granular, powder, fibrous, or multi-phase). In general, this transportation is done by a combination of mechanical, inertial, airflow, and gravity forces. Auger, belt, and slat conveyors mainly use mechanical forces. Oscillating conveyors use a combination of inertial and frictional forces. Pneumatic conveyors use air pressure and stream to transport materials. Materials can also be transported by launching, a method that involves using a combination of inertial and aerodynamic forces, as is the case in forage blowers (Behrouzilar, 2012).

2.6.1 Pneumatic conveying and separation

After examining the various options available for pod transport, it was decided that considering the flexibility needed in the machine, it is best to transport the product from the header to the tank by a pneumatic conveyor with the specifications discussed

to the pneumatic conveying system

After checking various types of conveyors available for pod transport, it was decided that considering the product, machine, and field conditions, the most fitting option would be to use a pneumatic conveying system. For optimal pod transport after harvesting, it was necessary to accumulate the pods in one place so as to minimize damage and avoid clogging other components (conveying tubes for example). Thus, an accumulation component (Figure 5) was designed to channel the product into an outlet, where they can be sucked into the conveying system.

below.

Pneumatic conveying systems can be divided into pressure systems, vacuum systems, and mixed systems, which are a combination of pressure and vacuum systems. A typical pneumatic conveyor system consists of an air mover component, a feeder component (where solid particles are mixed with air and transferred into the conveying line), a conveying line (a set of metal or plastic tubes that transport the mixture of air and solid particles from the origin to the destination), and a separation component responsible for separating solid particles from the air. Suction systems have a lesser impact on product quality than their equivalent pressure systems and can also be used to transfer materials from several origins to one destination. Since the goal was to build a small machine for harvesting, transporting, and storing the product, it was decided that a vacuum-type pneumatic conveying system would be superior to alternatives taking into account the product and field conditions. According to the gas laws, in a vacuum system, when the air pressure drops below the absolute pressure, the

air loses weight and its viscosity decreases, leading to reduced carrying capacity inside the pipe. On the contrary, when the tube pressure is greater than the absolute pressure, the air becomes heavier and therefore gains increased carrying capacity. Thus, pneumatic conveying is more of an experimental matter than a science.

One of the components commonly used in pneumatic conveying systems is the cyclone. A cyclone literally means a tornado with a low-pressure center generated by centrifugal forces, which has lower pressures at smaller diameters. The pressure difference in tornadoes has been perhaps one of the main inspirations for the invention of cyclones as a means of material separation (Wang, 2004). The purpose of a cyclone in a harvester is to separate the harvested product from the air that sucks the product. This component plays a key role in the performance of the pneumatic system. After examining the relevant literature and the performance of different stripper headers, this system was designed for transporting products to the collection tank without using large and bulky conveyors.

2.7 Cyclone design

Typically, cyclone design starts by calculating the diameter of the cyclone and then continues by optimizing other parameters as a factor of cyclone diameter. The schematic diagram of the elements assembled together to form the cyclone is illustrated in Figure 6.

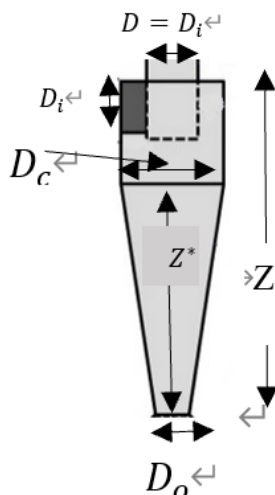


Figure 6 schematic diagram of the designed cyclone

Cyclone design Equation is equation(5).

$$\frac{D_c}{D_i} = 3 - 5 \quad \frac{Z^*}{D_i} = 5 - 10$$

$$D_o = D_i \quad \frac{Z}{Z^*} = 1.3 \quad (5)$$

Air movers commonly used in conveying applications include fans, blowers, and compressors. The insensitivity of centrifugal fans to air dust and their ability to move large volumes of air at low pressures in the range of 34.5 kPa make them an excellent choice for vacuum conveying systems. In tangential flow cyclones, the materials enter the cylindrical part tangentially and with an initial speed that gives them a rotational movement in the inner wall of the cylinder, where friction decreases their speed and the gravitational force drives them toward the solids outlet.

2.8 Conveying lines

The conveying lines for transporting the product from the centrifugal fan to the suction cyclone and from the accumulation component to the separation cyclone had to be flexible and strong enough to work with minimum loss. Also, the diameter of these lines had to be chosen such that the product can be optimally transported inside the tubes.

2.9 Pneumatic conveying system design

Considering the use of a centrifugal fan as the heart of the system, the required fan power had to be determined according to the product so that the fan would be powerful enough to generate the necessary suction for moving the product. This power was determined using Equation 6. Table 2 shows the pressure drop in some common components of the pneumatic conveying system.

$$P = \frac{\Delta P Q}{\eta_b} \quad (6)$$

In the above equation, P is the required fan power (Watt), ΔP is the pressure drop of the entire system (Pa), Q is the volumetric air flow rate ($\text{m}^3 \text{S}^{-1}$), and η_b is the power transmission efficiency, which is a function of the power transmission system.

As the fan power equation shows, to design a

pneumatic conveying system, first, the air velocity, air volume, total pressure drop, and the required fan power must be determined. The pressure drop in a conveying system is a set of terms given in the following equation.

$$\Delta P = \Delta P_L + \Delta P_a + \Delta P_s + \Delta P_g + \Delta P_b + \Delta P_c \quad (7)$$

where ΔP is the total pressure drop of the entire system (Pa), ΔP_L is the line pressure drop for air alone (Pa), ΔP_a is the pressure drop due to particle acceleration (Pa), ΔP_s is the pressure drop due to solids friction (Pa), ΔP_g is the pressure drop due to gravity (Pa), ΔP_b is the pressure drop in bends (Pa), and ΔP_c is the pressure drop in the components (Pa).

The line pressure drop is estimated by the following equation:

$$\Delta P_L = \lambda_1 \frac{\rho}{2} V^2 \frac{L}{D} \quad (8)$$

Where λ_1 is the friction loss coefficient, ρ is the air density (kg m^{-3}), V is the air velocity (m s^{-1}), L is the length of the conveying tube (m), and D is the tube diameter (m).

The friction loss coefficient for turbulent flows can be obtained from the following equation, where $N_{re} = \frac{\rho V D}{\mu}$ is the Reynolds number and μ is the air viscosity (Behrouzilar, 2012).

$$\frac{\lambda_1}{4} = 0.0024 + 0.125 N_{Re}^{0.32} \quad (9)$$

The pressure drop due to particle acceleration can be obtained from the following equation (Behrouzilar, 2012):

$$\Delta P_a = \phi_m V_p C \quad (10)$$

Where ϕ_m is the mass flow rate (dimensionless) and C is the velocity of solid particles (m s^{-1}).

Researchers have proposed the following equation for estimating C (Behrouzilar, 2012):

$$\frac{C}{v} = 100.68 d^{0.92} \rho_p^{0.5} \rho^{0.2} D^{0.54} \quad (11)$$

where d is the average particle diameter (m) and ρ_p is the specific mass of solid particles (kg m^{-3}).

The pressure drop due to solids can be estimated from the following equation.

$$\Delta P_a = \phi_m \lambda_s \frac{\rho}{2} V^2 \frac{L}{D} \quad (12)$$

Kono and Sito have proposed the following equation for estimating the solid friction coefficient, λ_s , for the above equation (Behrouzilar, 2012).

$$\lambda_s = \frac{0.0285 \sqrt{gD}}{c} \quad (13)$$

where g is the acceleration of gravity (9.81 m s^{-2}).

The pressure drop due to gravity (elevation) is given by Equation 14.

$$\Delta P_g = \rho^* g \Delta Z \quad (14)$$

where ΔZ is the elevation height (m) and ρ^* is the apparent specific mass of the solid (kg m^{-3}) in the conveyance process, which is calculated from Equation 15:

$$\rho^* = (\phi_m V_\rho) / C \quad (15)$$

The pressure drop in bends occurs because of the friction of the air and solids with the wall. This pressure drop is calculated separately for air and solids. The pressure drop due to air friction with the wall can be obtained from the equivalent length of the bend, i.e. the length of a straight pipe that produces the same pressure drop, which is given by the following equation.

$$L_{ep} = \frac{KD}{\lambda_1} \quad (16)$$

In this equation, K is the bend pressure loss coefficient, which can be obtained from Table 2. The equivalent lengths must be calculated for individual bends must be summed up to obtain the total pressure drop for all bends.

The pressure drop due to the fraction of solids with the wall is given by Equation 17:

$$\frac{\Delta P_{b \text{ solid}}}{\rho v^2} = 0.245 \frac{m^{1.267} R^{0.260}}{\rho v D^2 D} \quad (17)$$

where $\Delta P_{b \text{ solid}}$ is the bend pressure loss for solids (Pa) and $\frac{R}{D}$ is the ratio of the bend radius to the tube

diameter.

The pressure drop in each component depends on the shape and design of that component. While there is no specific formula for calculating this pressure drop, it can be estimated from the data provided in the literature. Manufacturers of parts usually report this pressure drop for their products. Table 2 shows the pressure drop in some common parts.

Table 2 Pressure loss coefficient (k) of some common parts for turbulent flow

K	Geometry/Shape	Part
0.5	Sharp	Inlet
0.005	Round	
0.38	Sharp ($\frac{D_2}{D_1} = 0.5$)	Stenosis
1.3	45° cut	bend ⁹⁰
0.9	Small radius	
0.6	Large radius	

2.10 Power transmission to components

An arrangement of belts and pulleys was used to transfer power from the machine to the components. The belt-pulley system is commonly used for mechanical power transmission under pure tension across relatively large distances between two parallel shafts with different RPMs. This system has several advantages over other means of mechanical power transmission, including cost-effectiveness, ability to absorb impact loads and vibrations, and

relatively good efficiency. Also, this system is a perfect choice for use in dusty environments. For these reasons, it was decided to use this power transmission system for preliminary assessments.

2.10.1 Determination of the theoretical distance between pulleys (machine to header and machine to centrifugal fan)

$$D_z < O < 3(D_z + D_1) \quad (18)$$

In equation (18), O is the experimental center-to-center distance of pulleys (mm), D_1 is the diameter of the smaller pulley (mm), and D_2 is the diameter of the larger pulley (mm).

2.10.2 Determination of belt length

The required belt lengths were determined using the following equation and then the belts were chosen according to the standard sizes available in the market.

$$L = 2O + 1.57(D_2 + D_1) + \frac{(D_2 - D_1)^2}{4O} \quad (19)$$

2.10.3 Center-to-center distance of drive-header pulleys and drive-centrifugal fan pulleys

$$O = \frac{B + \sqrt{B^2 - 32(D_2 - D_1)^2}}{16} \quad (20)$$

$$B = 4L - 6.28(D_2 + D_1) \quad (21)$$

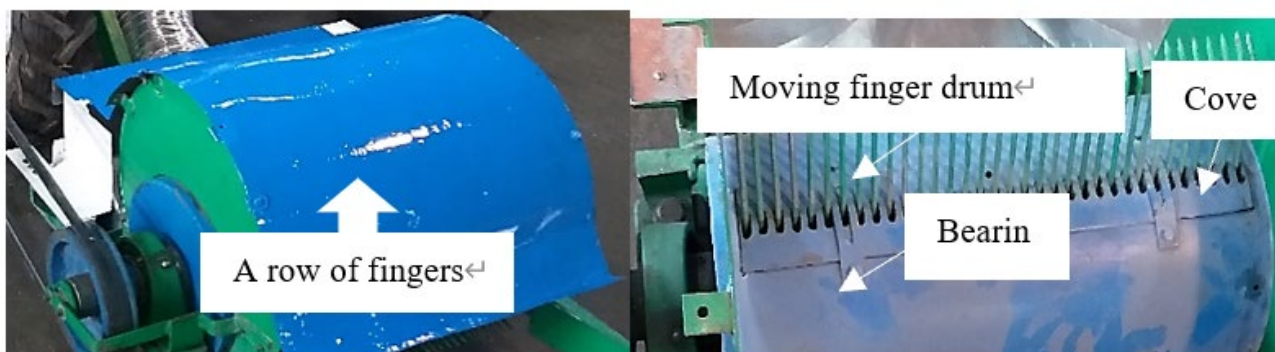


Figure 7 Diagram of the fabricated header and a row of fingers

3 Results and discussion

The components of the fabricated stripper header included a stripping unit and its drive system, a drum holding the fingers, side support plates, shoes, chassis, power source's drive system and reduction gears, product separation plates, pulley shafts for power transmission, and a cover (Figure 7).

The fingers were fitted inside drum holes with a diameter of 6 mm at a spacing of 7 mm for easier movement. The spacing between fingers was determined according to the size of chickpea pods and the characteristics of chickpea plants in field observations. Using the same data, it was decided to use 170 mm long fingers. The header was made with four rows of fingers, each row consisting of 34

fingers, with a working width of 570 mm and a drum diameter of 270 mm. The fingers' movement was a combination of a translational motion and a cam-like off-center rotational motion, forming a cycloidal path, in order to prevent fingers from hitting rocks, soil, and other unwanted materials.

3.1 Header performance

Given the dimensions of the header, its working width 570 mm, and the length of the finger touching the product 65 mm, the stripping area of one row of fingers was determined to be 37050 mm².

The preliminary assessment of the machine was conducted for the yield of 600 kg ha⁻¹, 25 plants per square meter, 10 seeds per plant, 1 seed per pod, 100-seed weight of 28 g, plant height of 30 cm, and the yield per square meter of 60 grams (Table 3). Thus:

$$\text{Number of seeds per square meter} = \frac{60 \times 100}{28} = 214.28 \quad (22)$$

$$\text{Number of pods in the stripping area} = \frac{37050 \times 214.28}{10^6} = 7.94 \quad (23)$$

The force needed for pulling the pods was determined using the static method:

$$7.94 \times 8.3 \text{ (N)} \approx 66 \text{ (N)} \quad (3)$$

The field capacity (the work done in one hour) was determined to be 0.0546 ha h⁻¹. The product inflow rate of each finger for a drum rotational speed of 15.7 rad s⁻¹ and RPM of 150, and the forward speed of 0.25 m s⁻¹ was determined to be 0.00294267. The product inflow rate of the machine at the same speed for a header width of 0.57 m and 10 stems per plant was calculated to 1.425 m² s⁻¹.

3.2 Product accumulator

Since the harvested product had to be accumulated in some place for better suction, a cuboid compartment with an inclined interior (Figure 8) was used for this purpose. The dimensions of this compartment were chosen such that it can work with all of the pods picked up by the fingers (Figure 8).

3.3 Cyclone

Considering the advantages, disadvantages, and limitations of each type of pneumatic conveying

system, a vacuum-type pneumatic conveying system was used in the machine. The cyclone of this system was designed according to Equations 5, which gave the following dimensions for its various components for $D_i = 15 \text{ cm}$ and $\frac{D_c}{D_i} = 3.3 : Z^* = 100 \text{ cm}$, $Z = 130 \text{ cm}$, and $D_o = 15 \text{ cm}$.

This cyclone was then modeled in SOLIDWORKS (Appendix A). Finally, the cyclone was fabricated from galvanized steel sheets with a thickness of 0.7 mm and sealed with silicone (Figure 9). Considering the size of this cyclone, it was placed on a surface mounted on the rear part of the machine chassis in order to prevent vibrations and avoid obstructing the driver's vision in the field.

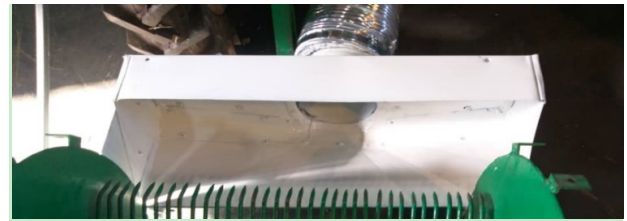


Figure 8 Product accumulator mounted on the header



Figure 9 fabricated cyclone mounted on the machine chassis

3.4 Calculation of pressure loss and centrifugal fan power requirement

The total pressure drop of the centrifugal fan was obtained for a specific mass of $\rho = 1400 \text{ kg m}^{-3}$ (for chickpeas) and the air velocity of 30 m s⁻¹ using the equations presented in the previous sections. The air velocity of 30 m s⁻¹ was chosen because the limit velocity may differ for different products.

$$\text{Volumetric air flow} = Q = \left(\frac{\pi}{4}\right)(0.15)^2(30) = 5.3 \text{ m}^3 \text{ s}^{-1} \quad (4)$$

$$\text{Mass air flow} = \rho Q = 1.2(0.530144) = 0.636173 \text{ kg s}^{-1} \quad (5)$$

(Specific mass of air = 1.2 kg m^{-3})

Based on these values, the Reynolds number was calculated to 5.4×10^{-5} .

Table 3 Rainfed and irrigated chickpea cultivation area in Iran based on the agricultural statistics of 2017-2018

Irrigated	Rainfed	Product: chickpeas
7248	572077	Area (hectares)
10989	274770	Production (tons)

As shown in Table 3, the rainfed and irrigated chickpea yield is $0.4803 \text{ ton ha}^{-1}$ and is $1.516 \text{ ton ha}^{-1}$, based on which the product conveying rate was calculated to 0.0073 kg s^{-1} and 0.023 kg s^{-1} respectively. Accordingly, the mass flow rate was calculated to 0.011 for rainfed fields and 0.036 for irrigated fields. Based on these values, the Reynolds number was calculated to 5.4×10^{-5} .

By substituting these values into equations, λ_1 was calculated to 0.031, and the line pressure drop was determined to be 334.8 Pa accordingly. The pressure drop due to particle acceleration (for pea pod with a geometric mean diameter of 8.3 mm) with $O=26.78265 \text{ m s}^{-1}$ was calculated to 10.6 Pa for rainfed fields and 34.71 Pa for irrigated fields. To obtain the pressure loss due to elevation, first, ρ^* was calculated to $0.01478 \text{ kg m}^{-3}$ and 0.048 kg m^{-3} for rainfed and irrigated conditions, then using these ρ^* values, this pressure drop was calculated to 0.29 Pa and 0.94 Pa for rainfed and irrigated conditions, respectively. Having $\lambda_s = 1.29084 \times 10^{-3}$, the pressure drop due to solids was determined to be 0.153 Pa and 0.502 for rainfed and irrigated conditions respectively. Assuming $K=0.9$ for bends, L_{eq} was calculated to 4.35484m for air and 8.70968m for solids. Accordingly, assuming $R/D=5$, the pressure drop due to the fraction of air and solids in the bends was determined to be 0.972 kPa and 7.223 Pa respectively.

Therefore, after adding all of the above pressure drops, the total pressure drop in the conveying process was determined to be 1325.066 Pa and 1350.175 Pa for rainfed and irrigated conditions respectively. Based on these results, the power

required for conveying chickpeas was calculated to 1.17162 kW and 1.19282 kW for rainfed and irrigated conditions respectively. Since the machine was expected to harvest several varieties of legumes, it was decided to use a centrifugal fan with a power of 5 HP at 3000 RPM (Figure 10) to ensure it operates at the expected efficiency level with a good safety margin.



(a) Centrifugal fan



(b) Fan installation location

Figure 10 Fan information

3.5 Power transmission

The designed and fabricated machine gets all of its required power from a BCS harvester with a 12.5 HP engine, which meets the size and power requirements (Anonymous, 2015). The maximum RPM of the engine is 3000 rpm. The generated power goes through a 3-to-1 reduction gear, arriving at a PTO shaft (at 1000 rpm according to the engine's catalog). This power was transferred to the stripper header and centrifugal fan through a system of pulleys and belts. Because of geometrical limitations, the experimental center-to-center distance of drive-header pulleys and drive-centrifugal fan pulleys was set to 650 mm and 480 mm respectively. The pulley used on the drive shaft was a standard pulley with a diameter of 30 cm (Figures 11). For the centrifugal fan, this pulley was connected to another pulley with

a diameter of 10cm giving a 1-to-3 RPM conversion (Figures 11). Since the header needed a lower RPM, it was fitted with a pulley with a diameter of 8 cm, and a groove was cut on the 30 cm pulley to reach an 8-to-20 conversion. V-shaped type-B belts of appropriate lengths were fitted on the pulley systems. The appropriate best length was determined to be 76.51 in for drive-header pulleys and 55.47 in for drive-centrifugal fan pulleys. The actual center-to-center distance of drive-header pulleys and drive-centrifugal fan pulleys was determined to be 653.347 mm and 486.5 mm, respectively. Considering the relatively large distance between the drive and centrifugal fan pulleys, a tensioner pulley was placed between them to ensure maximum belt-pulley contact. The position of this tensioner pulley was chosen so that it can be adjusted for the appropriate level of belt-tightening to avoid derailment.



(A) drive-centrifugal fan pulley



(B) drive-header pulley

Figure 11 pulleys

Collapsible hose tubes made of aluminum with a diameter of 15 cm were used to transport the

harvested product from the header by suction. These tubes were chosen because of their appropriate flexibility and thickness for preliminary assessments. These tubes were fixed to the machine by metal fasteners to avoid any issues during the operation.

After designing and fabricating or purchasing the needed parts, assembling the machine on a BCS harvester (Appendix B), and painting the surface, the machine was tested under laboratory conditions.

4 Conclusion

For the preliminary assessment of the header, first, a series of chickpea plants were fed to the header from near the ground (simulating the way the header would pick the plants in the field) to determine whether it works as intended. It was observed that the header was able to collect and separate the pods from the plant and pour them into the accumulation component. As explained in previous sections, the inclinations embedded in this component guided the product toward the tube, where it was sucked into the next component. Then, for the initial evaluation of the cyclone and centrifugal blower, three groups of 35 chickpea pods were separated by hand and entered the concentrator, and the motor speed of the BCS machine was experimentally set at three different speeds: low (454 RPM according to the catalog), medium and maximum (3000 RPM according to the catalog) was changed by hand, by manual gas and it was observed that initially the suction of the centrifugal blower is relatively high due to the distance of the cyclone from the concentrator and a number of pods inside the hose that transports the product to The side of the cyclone carries, remains, and then at medium speed, this drop is reduced, and at medium to high speeds, the product is completely sucked into the cyclone without any drop. According to the observations in the preliminary evaluations given in Table 4, it shows that if the car performs better with medium to high revs.

The initial evaluations showed that the built machine can transfer the necessary power to the

centrifugal blower and the header, and the header can remove the desired product pods without any problems, and the harvested pods are concentrated in the desired location to be sucked by the centrifugal blower and removed. Separation from air is done through a cyclone.

Table 4 Machine performance at different engine speeds (RPM)

Product collected (%)	Feed size (number of plants)	Engine speed (RPM)
		454 rpm
30%	10	r_1
20%	10	r_2
25%	10	r_3
		3000 rpm
97%	10	r_1
100%	10	r_2
100%	10	r_3

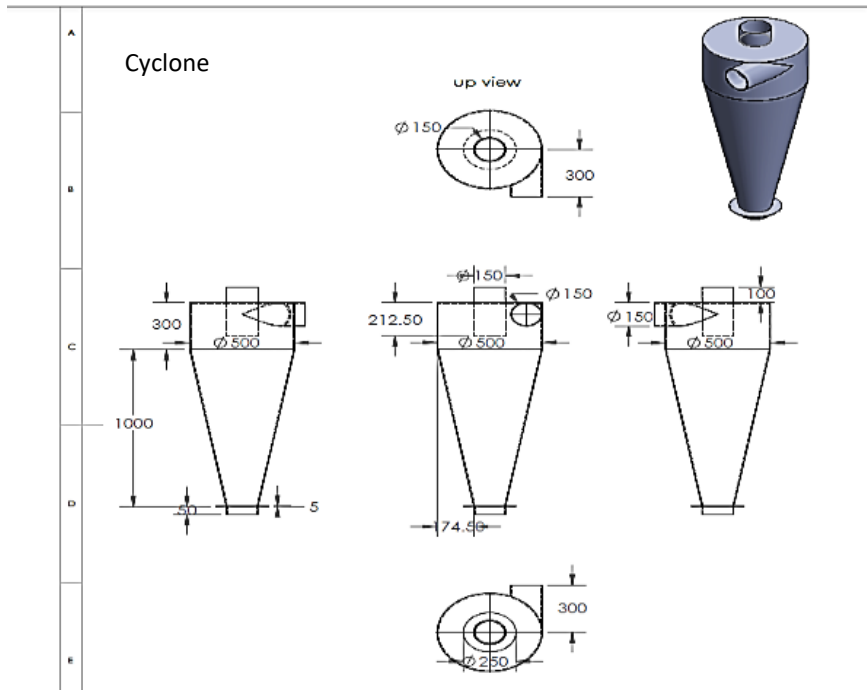
5 Acknowledgments

The authors thanks University of Tabriz for supporting this project.

References

- Abdullapour and Salimi. 2017. Measurement of Static and Dynamic Shearing Resistance of Agricultural Products. M.S. thesis, Biosystem Mechanics, Department of Biosystem Engineering, Faculty of Agriculture, University of Tabriz, Tabriz, Iran.
- Anonymous. 2015. Manual for BCS 622 Harvesters Manufactured by Sabz Kush Negin Co.
- Arianpour, A. 2013. "Assessment Standards for the Agriculture Profession." Educational Research and Planning Organization. Department of Textbook Planning and Composition for Technical-Vocational/Professional and Manual Skills Fields. Publication Year: 2014.
- Behrooz-Lar, M., and B. K. Huang. 2002. Design and development of chickpea combine. *Agricultural Mechanization in Asia Africa and Latin America*, 33(1): 35-38.
- Behrouzilar, M. 2012. Design Principles of Harvesting Machines and Material Transport Systems. Gholami Publications. Vol 3.
- Bhanage, G. B., P. U. Shahare, V. V. Aware, and J. S. Dekhale. 2017. Development and paddy stripping header mechanism. *International Journal of Agricultural Engineering*, 10(1): 179-185.
- Chico-Santamarta, L., H. Masebu, D. R. White, R. J. Godwin, and M. Crook. 2013. The development of an improved stripping mechanism for sorghum harvesting. ASABE Paper No. 131620136. Kansas City, Missouri: American Society of Agricultural and Biological Engineers (ASABE).
- Firozi, A. 2018. Dynamic and kinematic study of the product in a laboratory stripper combine. M.S. thesis, Department of Agricultural Technical Engineering, Aburaihan Campus, University of Tehran, Iran.
- Han, B., W. Wu and X. Huang. 2010. Experiments on design parameters of stripping header for super rice in cold region. *Transactions of the Chinese Society of Agricultural Engineering*, 26(12): 125-130.
- Jiang, Y., J. Xu, H. Zhang, E. Jiang, C. Tu, P. Luo, J. Wang, T. Li, Y. Ma, and J. Qu. 2001. Rice (wheat) combine harvester with cutting and windrowing straw immediately after stripping. *Transactions of the Chinese Society of Agricultural Engineering*, 17(1): 64-68.
- Khojamli, R. 2016. Design, fabrication, and evaluation of a laboratory model of a wheat stripper header equipped with a threshing unit. M.S. thesis, Department of Agricultural Technical Engineering, Aburaihan Campus, University of Tehran, Iran.
- Koochaki, A., and M. Bannayan. 1986. Cultivation of Legumes, Javid Publications.
- Metianu, A. A., O. D. Hale and R. N. Hobson. 1991. Review of grain harvesting research and development at Silsoe. In *Proc. of the International Agricultural Mechanization Conf.*, 124-148. Beijing, China, 16-20 October.
- Tado, J. M. C. 1992. Field testing of IRRI rice stripper harvester. Rome, Italy: FAO.
- Tavakkoli Heshtjin, T., Golpira, H., Khoshtaghaza, M. H., and Minayi, S. 2009a. Determination of some mechanical properties of chickpeas for use in the design of chickpea harvesting machines. *Journal of Agricultural Science*, Volume 19, No2.
- Tavakkoli, H., Mohtasebi, S.S. & Jafari, A. 2009b. Effect of Moisture Content and Loading Rate on the Shearing Characteristics of Barley Straw by Internode Position, *Agricultural Engineering International*, the CIGR Ejournal, Manuscript 1176. Vol. XI., March
- Wang, J. 2004. Theoretical study of cyclone design. Ph.D. diss., Biological & Agricultural Engineering, Texas A&M University.
- West, N. L., and E. C. Lundahl. 1986. Harvesting machine for stripping seeds from a standing crop. US Patent No. 4578934 (In USA).

Appendix A



Appendix B

